

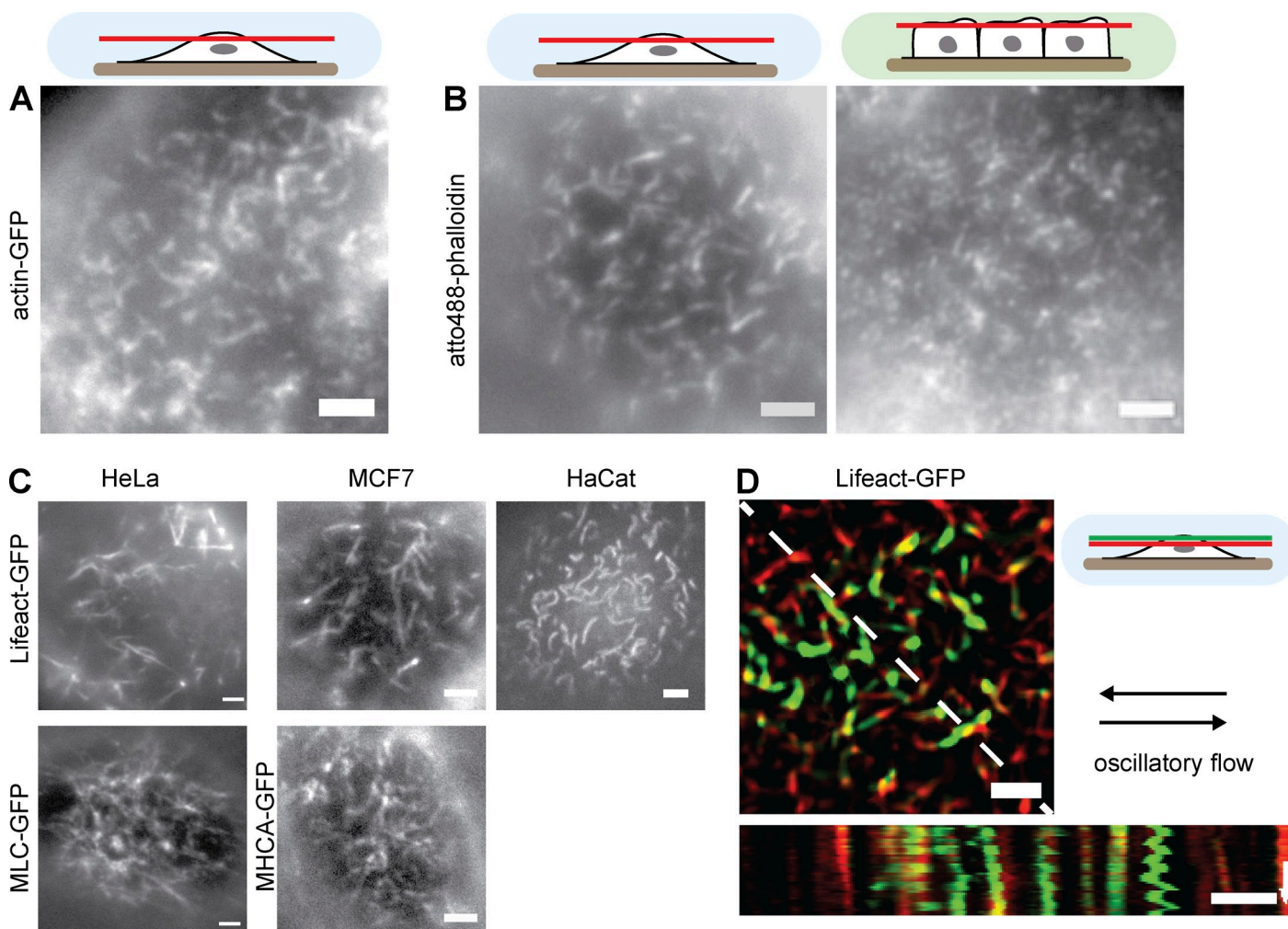
Klingner et al., <http://www.jcb.org/cgi/content/full/jcb.201402037/DC1>

Figure S1. **Apical actin and myosin organization.** (A and B) MV in nonconfluent (A and B, left) and confluent (B, right) MDCK cells, labeled with actin-GFP (A) or Atto488-phalloidin (B). (C) Apical actin and myosin organization in selected EC lines. (D) Exposure of MDCK cells labeled with Lifect-GFP to oscillatory flow. Kymograph (dotted line) shows movement of protruding MV (zigzag lines) as well as immobile (smooth lines) actin structures. Bars, 2  $\mu$ m. Time arrow, 20 s.

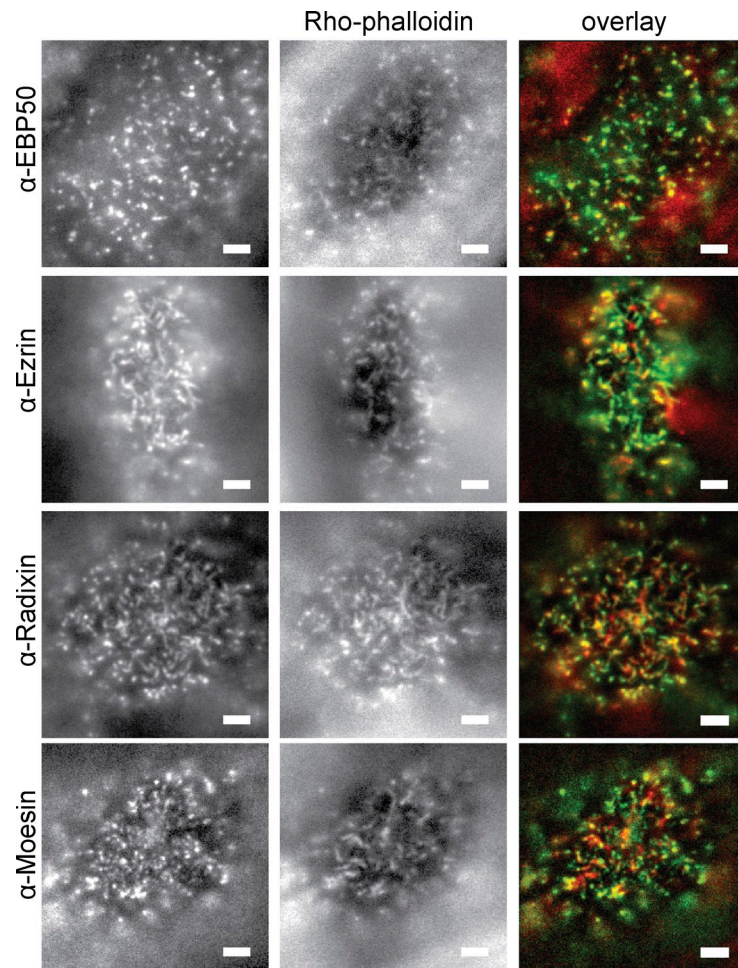


Figure S2. **Colocalization of actin with ERM proteins.** Immunofluorescence labeling of selected MV marker proteins. EBP50 serves as a membrane anchor for the ERM family proteins ezrin, radixin, and moesin. Actin was stained with rhodamine (Rho)-phalloidin. For colocalization, images were background subtracted using a Fiji plugin before color overlay. Bars, 2  $\mu$ m.

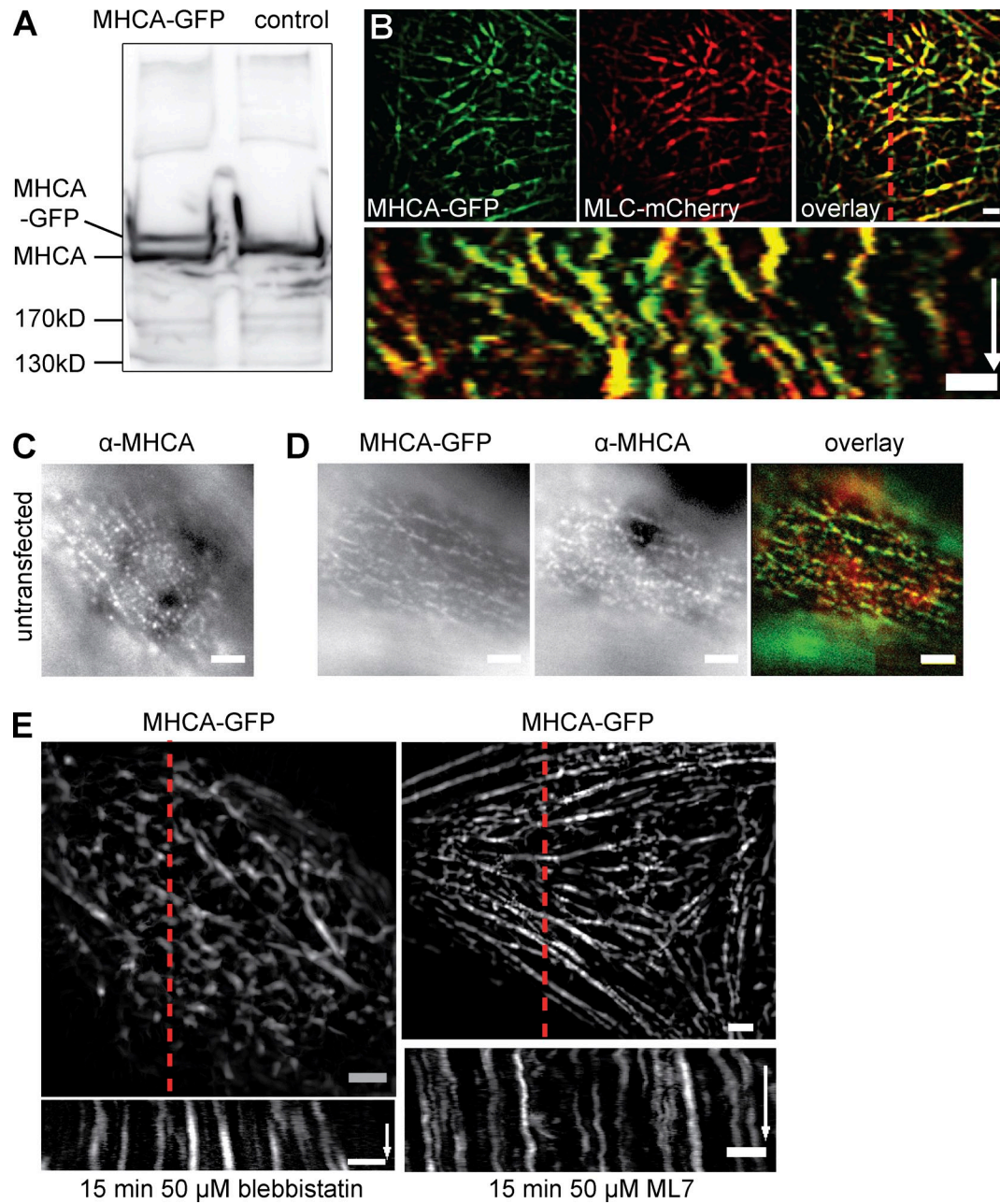


Figure S3. **Characterization of myosin markers.** (A) Western blot of cells stably transfected with MHCA-GFP versus control MDCK cells, using an anti-MHCA antibody (marker bands and target bands indicated). (B) Cell stably transfected with MHCA-GFP and MLC-mCherry to confirm functionality and correct localization of myosin components. Kymograph demonstrates colocalization and joint dynamics. (C) Control MDCK cells stained with anti-MHCA antibody to demonstrate the presence of the isotropic network. (D) Stably transfected MHCA-GFP cell lines were stained with anti-MHCA antibody. Colocalization of the antibody signal with GFP fluorescence confirms correct localization of the MHCA-GFP protein construct. (E) Inhibition of myosin II function by blocking of myosin ATPase activity (blebbistatin) or inhibition of MLC kinase (ML7). In both cases, myosin dynamics is strongly reduced as depicted in the kymographs. Kymographs were taken along the indicated red dotted lines. Bars, 2  $\mu$ m. Time arrows, 300 s.

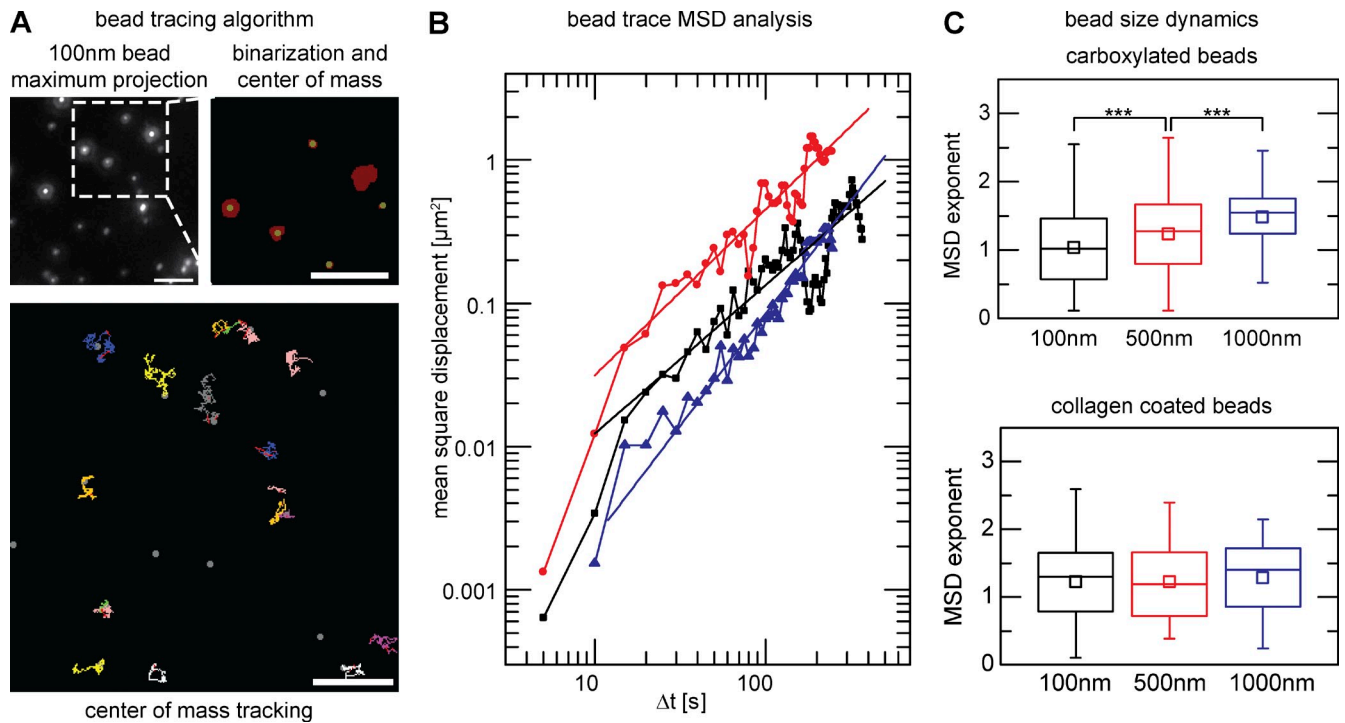


Figure S4. **MSD analysis.** (A) Overview of bead tracing algorithm before MSD analysis. Three successive image planes ( $\Delta z = 1 \mu\text{m}$ ) per time point were maximum projected and binarized (red objects) using adaptable threshold values. For each object within a defined maximum size, the center of mass was calculated in MATLAB (yellow dots) and traced using the ImageJ Plugin Particle Tracker (Sbalzarini and Koumoutsakos, 2005). Bars,  $5 \mu\text{m}$ . (B) Three examples of MSD fitting to particle traces with various MSD exponents (black: 1.0; red: 1.2; blue: 1.6). Colored lines represent linear fits to the data points. (C) MSD analysis for beads of various dimensions reveals change from diffusive motion to active transport caused by steric effects for carboxylated beads (same data as in Fig. 8 D; black: 7 cells,  $n = 422$  beads; red: 6 cells,  $n = 335$ ; blue: 5 cells,  $n = 124$ ), whereas collagen-coated beads are actively driven irrespective of bead size (same data as in Fig. 8 D; black: 11 cells,  $n = 426$  beads; red: 8 cells  $n = 19$ ; blue: 5 cells,  $n = 16$ ). Results are given as box plots marking 25–75 percentile (boxes), median (lines), and mean value (small boxes). Whiskers indicate range of data points.

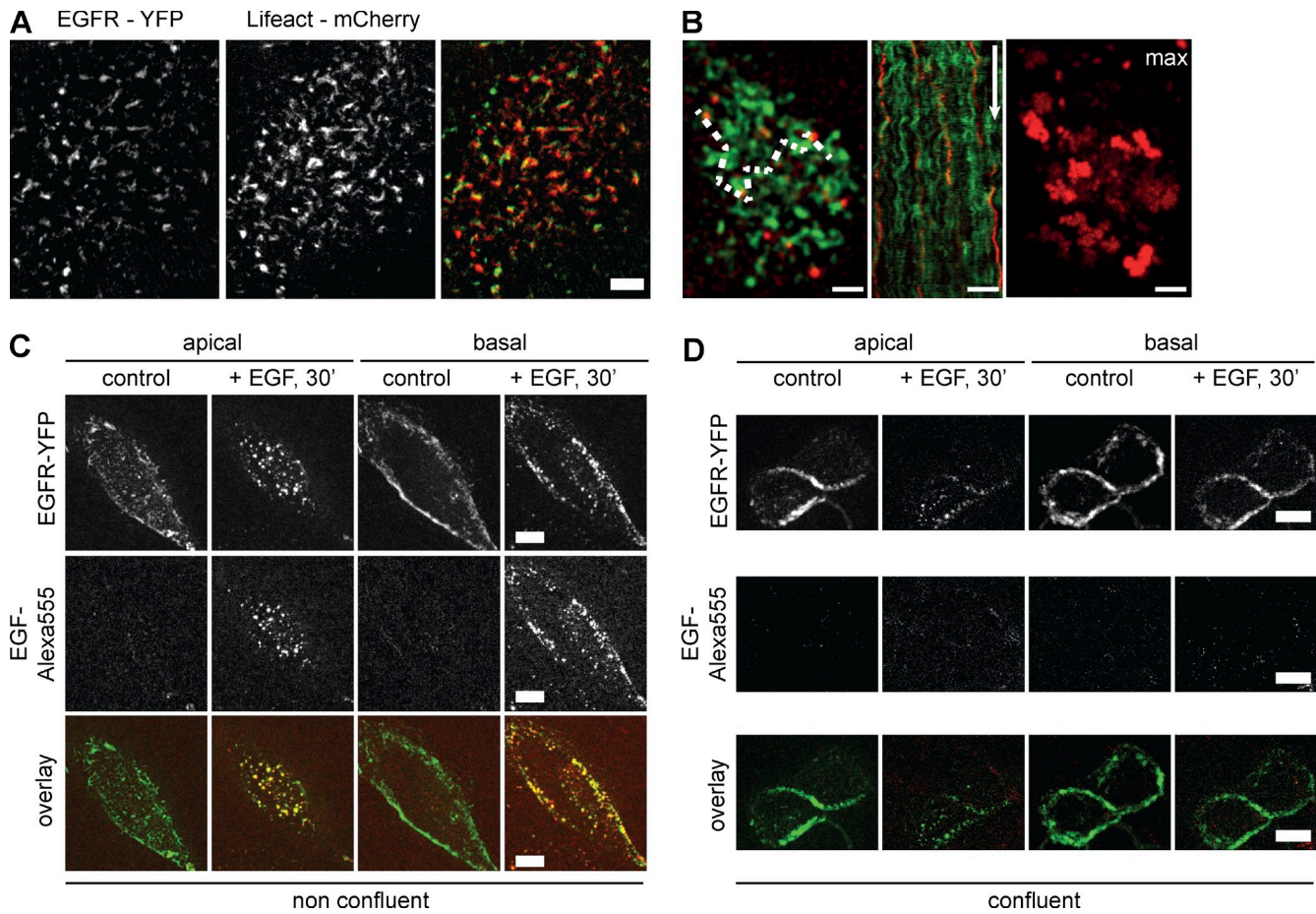
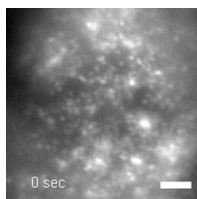
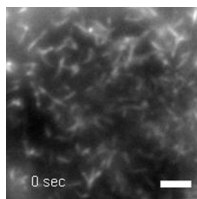


Figure S5. **Distribution of EGF and EGFR.** (A) EGF receptor (EGFR; EGFR-YFP) colocalizes with apical MV (Lifeact-mCherry) in nonconfluent MDCK cells. (B) Guided motion of EGF-Atto 488 (red) bound to the apical surface. Kymograph was created along the dotted line. Isotropically oriented movement through actomyosin dynamics (Lifeact-RFP in green) resulted in distribution of EGF over confined regions (max, maximum). Time arrow, 200 s. (C) Uptake of EGFR-YFP in nonconfluent cells upon adding EGF-Alexa Fluor 555. 30 min after EGF addition, EGFR was found in endocytic structures close to apical and basal surfaces (maximum projections: three planes;  $\Delta z = 1 \mu\text{m}$ ), where it colocalizes with EGF-Alexa Fluor 555. (D) Localization of EGFR-YFP at apical and basal surfaces of confluent MDCK cells. Maximum projections of three planes with  $\Delta z = 1 \mu\text{m}$ . EGFR localizes to lateral surfaces, and addition of EGF does not result in EGFR internalization. Bars: (A, C, and D)  $5 \mu\text{m}$ ; (B)  $2 \mu\text{m}$ .



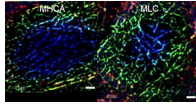
Video 1. **MV dynamics in confluent cells.** Time-lapse epifluorescence microscopy on a customized iMIC setup (FEI) of the apical cortex region of a confluent MDCK cell that has been stably transfected with Lifeact-GFP to label actin. Bar,  $2 \mu\text{m}$ . Frames were taken every 10 s for 10 min. Video to Fig. 3 A.



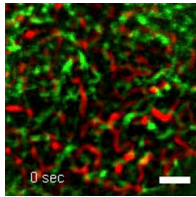
Video 2. **MV dynamics in nonconfluent cells.** Time-lapse epifluorescence microscopy on a customized iMIC setup (FEI) of the apical cortex region of a nonconfluent MDCK cell stably transfected with Lifeact-GFP to label actin. Bar,  $2 \mu\text{m}$ . Frames were taken every 10 s for 10 min. Video to Fig. 3 B.



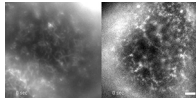
Video 3. **MV reorganization.** Time-lapse epifluorescence microscopy on a customized iMIC setup (FEI) showing examples of MV reorganization events in nonconfluent MDCK cells stably transfected with Lifeact-GFP: (1) bending, (2) exchange of connectivity, (3) flickering, and (4) lateral translation. Bar, 2  $\mu\text{m}$ . Frames were taken every 10 s for indicated times. Red asterisks, arrowhead, and circles indicate ends of filaments described in the respective panels. Video to Fig. 3 (D–G).



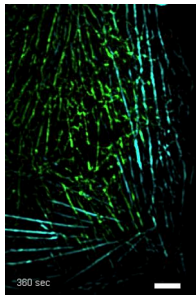
Video 4. **Myosin dynamics.** Time-lapse epifluorescence microscopy on a customized iMIC setup (FEI) showing isotropic reorganization of the apical myosin network in nonconfluent MDCK cells stably transfected with MHCA-GFP or MLC-GFP. Two focal planes ( $\Delta z = 1 \mu\text{m}$ ) were maximum projected and color coded in red (most basal) followed by green and blue (most apical). Bars, 2  $\mu\text{m}$ . Frames were taken every 10 s for 15 min. Video to Fig. 5 (E and F).



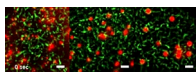
Video 5. **Actin-myosin colocalization.** Time-lapse epifluorescence microscopy on a customized iMIC setup (FEI) of a nonconfluent MDCK cell double transfected with MHCA-GFP and Lifeact-mCherry. Bar, 2  $\mu\text{m}$ . Frames were taken every 10 s for 15 min. Video to Fig. 6 A.



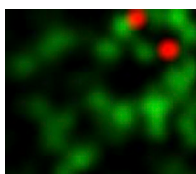
Video 6. **Disruption of the cell cortex.** Time-lapse epifluorescence microscopy on a customized iMIC setup (FEI) showing disruption of the apical MV array (left, cells stably transfected with Lifeact-GFP) and myosin network (right, cells stably transfected with MHCA-GFP) at the apical surface of MDCK cells, upon treatment with 2  $\mu\text{M}$  latrunculin A. Maximum projections of three (for actin,  $\Delta z = 1.5 \mu\text{m}$ ) or two (for myosin,  $\Delta z = 1 \mu\text{m}$ ) focal planes are shown. Bar, 2  $\mu\text{m}$ . Frames were taken every 20 s for 15 min. Video to Fig. 7 (A and B).



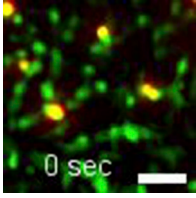
Video 7. **Unbalanced dynamics of myosin.** Time-lapse epifluorescence microscopy on a customized iMIC setup (FEI) of a MDCK cell stably expressing MHCA-GFP, treated with 500 nM latrunculin B. Green, myosin at apical plane. Cyan, myosin at basal plane. Bar, 5  $\mu\text{m}$ . Frames were taken every 10 s for 15 min starting 6 min after addition of latrunculin B. Video to Fig. 8 A.



Video 8. **Size-dependent confinement of beads.** Carboxylated red fluorescent polystyrene beads (red) of indicated size were monitored by time-lapse epifluorescence microscopy on a customized iMIC setup (FEI) at the apical surface of nonconfluent MDCK cells stably transfected with Lifeact-GFP (green). Bar, 2  $\mu\text{m}$ . Frames were taken every 2 s for 200 s. Video to Fig. 8 (B and C).



Video 9. **Trapping of carboxylated beads.** Carboxylated red fluorescent polystyrene beads (red) were monitored by time-lapse epifluorescence microscopy on a customized iMIC setup (FEI) at the apical surface of nonconfluent MDCK cells stably transfected with Lifeact-GFP (green). Frames were taken every 2 s for 200 s. Video to Fig. 8 B.



Video 10. **Trapping of collagen beads.** Collagen I-coated red fluorescent polystyrene beads (red) were monitored by time-lapse epifluorescence microscopy on a customized iMIC setup (FEI) at the apical surface of nonconfluent MDCK cells stably transfected with Lifeact-GFP (green). Bar, 2  $\mu\text{m}$ . Frames were taken every 2 s for 200 s. Video to Fig. 8 C.

**Code 1 shows object density analysis. A MATLAB code is provided for counting the number of objects per frame (flag list), object density (objects per image area), and bending parameter for each object with a skeleton length  $\geq 5$  pixels and  $\leq 4$  branching points.**

**Code 2 shows MSD analysis. A MATLAB code is provided using a trajectory report list from the ImageJ plugin Classic Particle Tracker to calculate the MSD for each bead trajectory longer than 30 frames. Curve fitting MSD exponent determination was then performed using Origin software.**

**Code 3 shows the image filtering procedure. A MATLAB code is provided that applies the Block Matching 3D algorithm followed by a local top-hat filter with Gaussian structure element.**

**Code 4 shows the bead image processing. A MATLAB code is provided for binarization of bead images using an adaptable threshold and subsequent determination of the center of mass for each identified object.**

**Code 5 shows the image reader. A custom algorithm is provided to create three-dimensional MATLAB matrices from LiveAcquisition TIFF images.**

**Code 6 shows image output. A custom algorithm is provided for converting three-dimensional MATLAB matrices into TIFF files.**

## Reference

Sbalzarini, I.F., and P. Koumoutsakos. 2005. Feature point tracking and trajectory analysis for video imaging in cell biology. *J. Struct. Biol.* 151:182–195. <http://dx.doi.org/10.1016/j.jsb.2005.06.002>